Journal of Computer-Aided Molecular Design, **12:** 37–51, 1998.
KLUWER/ESCOM

Charge distribution from a simple molecular orbital type calculation and non-bonding interaction terms in the force field MAB

Paul R. Gerber
Pharmaceutical Research and Development, F. Hoffmann-La Roche AG, Basel, Switzerland

Received 10 July 1997; Accepted 3 November 1997

Key words: charge distribution, dipole moment, force field, hydration, hydrogen bonding

Summary

A simple and fast method to calculate charge distributions in organic molecules is presented. The method is based on charge shifts within the saturated σ-system, driven by orbital electronegativities, coupled to a modified Hückel treatment of the unsaturated π-systems. Experimental molecular dipole moments of a set of 119 molecules are reproduced with a root mean square deviation of 0.36 Debye units. Furthermore, the obtained charge distribution is used to describe hydration free energies in terms of hydrogen-bonding donor and acceptor strengths of polar groups. Least square fitting to experimental data of 281 compounds leads to values for these strengths with accuracy limits of ±4.3% and ±2.5%, respectively. Properly normalized values are taken to parametrize the hydrogen bonding terms in our MAB force field. The method is sufficiently fast to be used in the preparatory phase of interactive force-field calculations.

Introduction

For large biomolecular systems theoretical modelling relies almost exclusively on force-field or molecular mechanics methods [1–8] because of their comparatively modest computational requirements. In most of these methods, assignment of partial atomic charges is one of the basic ingredients. In addition, the knowledge of the distribution of electric charge in a molecule is a key requirement for evaluating most of its physicochemical properties. With state-of-the-art quantum-mechanical methods charge distributions can in principle be calculated at any desired level of sophistication. However, for large systems the computational efforts become prohibitive. Therefore, the total charge distribution is approximated by additive schemes based on precalculated charge distributions of small building blocks. A standard procedure consists in deriving partial atomic charges for these subunits by optimally fitting the electrostatic potential to the one obtained from a full quantum mechanical treatment [9]. The fitting of the electrostatic potential is commonly (though not necessarily correctly) restricted to the external regions of the molecules.

An alternative and much less elaborate method consists in levelling out orbital electronegativities among the bonding atomic orbitals of a molecule [10–13]. This more heuristic approach has the additional advantage of producing conformation independent atomic charges. In a whole suite of models Abraham and co-workers have refined this approach to also include the effects of π-systems by performing a preceding Hückel calculation to obtain π-charges and by including by introducing polarization effects over several bonds [14,15].

Standard molecular mechanics calculations proceed by evaluating electrostatic interactions between the atomic point charges as the principal term of interaction between molecules. However, for hydrogen-bond acceptors there is both experimental and theoretical evidence for pronounced directionality [16,17], which seems difficult to reconcile with spherical potentials of atom-centered charges alone. Consequently, various additional force field terms have been proposed to account for the pronounced angular dependences of hydrogen bond interactions [18–21]. In particular, our own force field, MAB [22], attempts to account for the electrostatic interactions of polar

groups entirely on the basis of geometric hydrogen-bonding terms. In contrast to the assignment of partial atomic charges, the quantification of these heuristic hydrogen bonding terms is not standardized, although quantum chemical methods can certainly provide data for specific situations. The present work proposes a fast and reliable method for this purpose.

Simplified molecular orbital calculation

We envisage a simplified treatment of the electronic properties of a molecule by starting from the commonly used separation into a saturated (σ) part and (several) unsaturated (π) regions. For the σ-system a stationary solution of a charge transfer equation along bonds is used, without referring explicitly to electronic wave functions. In contrast, the π-systems are treated quantum mechanically, though with one of the simplest possible approximations, the Hückel method [23]. In addition, we allow both systems to influence each other via the charges accumulated at the atomic centers.

Treatment of the saturated (σ) part

The calculation of charge shift along bonds by levelling out atomic orbital electronegativities has a long tradition [10,24]. We make use of these ideas by setting up the following equations for electronic charge shifts along the directed σ-bonds

$$Ec_\beta = \sum_i \Delta_\beta^i \epsilon_i^\beta - Q \sum_i \Delta_\beta^i q_i, \qquad (1)$$

where c_β is the charge shift along the directed bond β, ϵ_i^β is the electronegativity of the orbital of atom i which forms the σ-bond, q_i is the atomic charge of atom i, and E and Q are free parameters. For each bond an arbitrary direction is predefined, and the quantity Δ_β^i is equal to 1, –1, or 0 depending on whether atom i is at the head of, the tail of, or not adjacent to bond β.

These equations, one for each bond β, are coupled through the atomic-charge balance equations

$$q_i = p_i + \sum_\beta \Delta_\beta^i c_\beta \qquad (2)$$

in which p_i is the π−, or formal charge of atom i.

In the process of parameter optimization it proved advantageous to reduce the value for the parameter Q in Equation (1) by a factor R for p type charges, Equation (2), as compared to the charges originating from the bond charge shifts c_β.

For the orbital electronegativities ϵ the experiment-based values of Hinze and Jaffé [25] were taken, which were suitably adjusted for the orbital s-character.

We have also considered to replace the constant E by more sophisticated expressions, such as derivatives of the orbital electronegativities [13, 24]. However, such modifications did not lead to significant improvements of the model.

Hückel calculation for unsaturated (π) regions

The basic treatment of the π-systems follows closely the Hückel-type calculation described earlier [22]. The main difference is that values for the diagonal elements of the Hückel matrix were also taken from the corresponding electronegativity values of Hinze and Jaffé [25] instead of being treated as free parameters. We described earlier [22] a self-consistent treatment which modulated the off-diagonal elements of the Hückel matrix with the resulting bond orders, leading to a more realistic description of conjugation effects. In the present treatment this self-consistency scheme, treating each π-system separately, has been abandoned in favor of an integrated overall feedback loop which also included the mutual influence of σ- and π-systems through the interaction terms of Equation (2) and the ones described in the following paragraph.

σ – π *Interaction*

As already stated in Equations (1) and (2) the charges resulting from the Hückel π-system calculation enter the equations of σ-bond charge shifts. Vice versa, the Hückel calculation can also be augmented by introducing additional diagonal terms in the Hückel-matrix, accounting for the influence of partial atomic charges. When restricted to π-systems alone, with the atomic charges originating from the previous round of Hückel-matrix diagonalization, this method is known as ω-technique [26]. In our case we modify each diagonal element α_i of the Hückel matrix by adding to the bare values α_{0i} an atomic charge term which also includes the charges accumulated through the σ-system charge shifts:

$$\alpha_i = \alpha_{0i} + \omega[p_i + R(q_i - p_i)]. \qquad (3)$$

In this expression ω is a free parameter and R was taken to be identical with the reduction factor introduced after Equation (2). This rather obvious choice

was adapted after exploratory calculations using an independent parameter.

With Equations (2) and (3) the Hückel and the σ-system charge-shift calculations influence each other. An overall solution can be obtained by iteratively treating the σ- and π-systems to achieve self-consistency.

The free parameters were adjusted to optimally reproduce experimental dipole moments as described in the next section.

Charge distribution and dipole moments

Atomic partial charges are directly derived from solving Equations (1) and (2) and from a population analysis of the Hückel result. They contribute the point-charge part p_{pc} to the molecular dipole moment:

$$p_{pc} = \sum_{i}^{atoms} q_i r_i, \qquad (4)$$

where $\mathbf{r_i}$ is the positional vector of atom i.

In addition, hybridization of atomic orbitals may contribute sizeable amounts to the molecular dipole moment [27]. In our simple molecular orbital description these contributions originate exclusively from the σ-system and can be estimated from the s-character of the hybridized atomic orbitals that participate in σ-bonds.

If all atomic σ-orbitals were occupied by two electrons the corresponding dipole moment would vanish. Thus, the population deficit from two electrons in each atomic σ-orbital yields a contribution to the atomic hybridization dipole moment. (We prefer this deficit-type view because lone pairs are much more frequent in our systems than empty orbitals.) The hybridization contribution p_{hi} of atom i to the molecular dipole moment can then be taken to be proportional to:

$$p_{hi} = \sum_{\beta}^{\sigma-bonds} \sqrt{(s^i_\beta(1 - s^i_\beta))(1 + \Delta^i_\beta c_\beta)}\mathbf{v}_\beta, \qquad (5)$$

where s^i_β is the *s*-character of the orbital of atom i which participates in bond β. To arrive at a properly dimensioned quantity, p_{hi} is multiplied by the van der Waals radius ρ^{vdW} of the atom and by a quantity P_h, which is the norm of the matrix element of the electronic position vector between *s* and *p* orbital [27] taken in units of ρ^{vdW}. The direction of the dipole contribution of a bond is given by the unit vector $\mathbf{v}_\beta$ pointing along the bond β, away from atom i. The quantity P_h is treated as a free parameter, independent of the atom group but different for different rows of the periodic system.

The s-character of the atomic σ-orbitals was taken to be related to the state of hybridization, reduced by a factor dependent on group and row of the element:

$$s^i = \frac{f^i}{h^i + 1}, \qquad (6)$$

where the hybridization number h is equal to 3, 2, and 1 for sp_3, sp_2, and sp_1 hybridizations, respectively. For the reduction factors f^i we took 0.88 and 0.42 for atoms O and F, respectively, and 1.0 for the remaining first row elements. For higher-row elements the values for f^i were reduced by a factor of 0.32 per row. Such values were suggested by considering bond angles of suitable compounds.

Comparison with experiments

A set of 119 neutral molecules with well defined geometries [28] and known dipole moments [29] was used to obtain values for the model parameters $E = 16$ eV and $Q = 22$ eV of Equation (1), $R = 0.61$ and $\omega = 0.64$ of Equations (2) and (3), and $P_h = 0.275$ and 0.487 for first and second row elements, respectively, Equation (5). Comparison of the calculated dipole moments with experimental ones is shown in Figure 1 and listed in Appendix 1. The root mean square deviation of 0.36 Debye units can be interpreted as an indication that the model provides a fairly satisfactory description of molecular charge distribution. Modern semi-empirical quantum-mechanical methods lead to dipole moment values of comparable accuracy (0.3 Debye in [30]), while high-level *ab-initio* calculations produce considerably better values. The values for the parameter P_h are of acceptable size, when compared to estimates with hydrogen-atom-type wave functions.

Charge distribution and free energy of hydration

The aim of this section is to make use of the charge distribution calculation of the previous sections to parametrize the non-bonded interactions in our force field MAB. To that end we try to relate the charge distributions to experimental data of the free energy of hydration of small compounds, of which a large amount has been compiled [31]. Free energy data seem to be particularly suited for that purpose, because

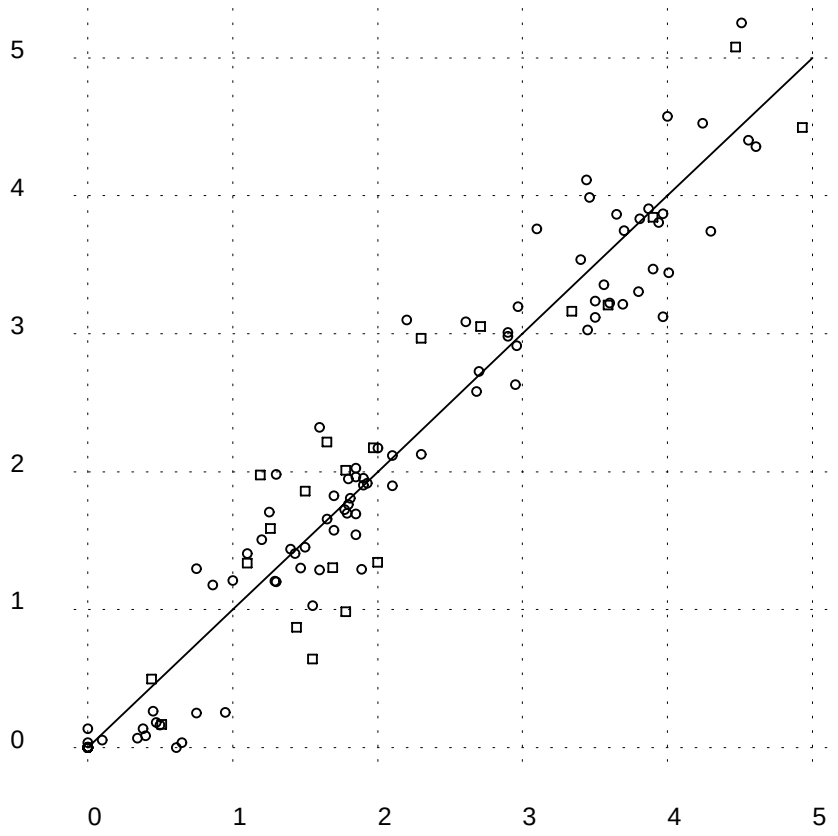

Figure 1. Calculated versus experimental dipole moments (in Debye units) of 119 neutral molecules. The rmsd is 0.357 Debye.

these are available for more compounds than, e.g., enthalpy data. Furthermore, they show little variation with molecular size so that functional group effects show up rather clearly.

We emphasize that the following models aim principally at finding an atom-based formulation which lends itself to automatic parameter assignments without the need to resort to prior identification of functional groups, with all its problems and limitations. Consequently, the introduction of any descriptors to fine-tune the agreement with experiment is avoided in favor of unraveling atomic hydrogen-bonding properties.

Hydrocarbons

Before we can proceed to analyze the polar contributions to the Gibbs free energy of hydration, we must first find a description suited for apolar compounds. To this end we consider for the moment only the hydrocarbons from the table of Appendix 2. For these compounds the experimental values of the Gibbs free energy of hydration ΔG_h can be reproduced rather satisfactorily by the following simple five-parameter model:

$$\Delta G_h^a = g_0 + g_s N_s + g_r N_r + g_\pi^2 N_\pi^2 + g_\pi^1 N_\pi^1, \quad (7)$$

where the superscript a indicates the apolar contribution. The descriptors N are defined a follows.

The topological surface number N_s is a sum over atom contributions N_s^i

$$N_s^i = 4\pi(\rho_i^{vdW})^2 \left(1 - \frac{n_l}{h^i + 1}\right), \quad (8)$$

where n_l is the number of ligands of atom i. The corresponding parameter g_s has a value of 0.031 ± 0.004 kJ/mol per Å^2. This value compares well with the corresponding atom-solvation parameter of aliphatic carbon [32].

The ring number N_r is also taken as a sum over single-atom quantities N_r^i which have the value of $1/l_s^i$,

where l_s^i is the size of the smallest ring to which atom i belongs. For atoms which are not members of a ring we have $N_r^i = 0$. Thus, for simple systems N_r is precisely the number of rings. Correspondingly, the parameter $g_r = -4.39 \pm 0.34$ kJ/mol is consistent with analogous parameters in alternative models [33].

The descriptors N_π^k count the number of π-orbitals for sp_k-hybridized atoms ($k = 1, 2$). The corresponding parameters have the values $g_\pi^2 = -1.29 \pm 0.06$ and $g_\pi^1 = -1.82 \pm 0.11$ kJ/mol. Finally, the constant g_0 assumes a value of 5.53 ± 0.52 kJ/mol.

The comparison of the calculated values with the experimental ones is shown in Figure 2. For these apolar compounds, which cover an rmsd range of 1.3 ± 7.8 (rmsd) kJ/mol, the model yields values with a root mean square deviation of 1.2 kJ/mol from the experiment. We consider this as quite satisfactory.

Polar compounds

Contributions to the Gibbs free energy of hydration of polar groups are considerably larger than the variation of 7.8 kJ/mol, found in the class of hydrocarbons, discussed in the previous section. Thus, we will keep the descriptors of the previous section together with parameter values and add a few additional terms characteristic for the polar atoms. With the aim to attribute these terms to hydrogen-bonding capabilities of the groups we attempt to define hydrogen-bonding atomic donor- and acceptor strengths in accordance with the concept of the hydrogen-bonding term in the energy expression of our MAB force field [22].

Thus, we attribute to each polar hydrogen a hydrogen-bonding donor strength determined by its structural context within the molecule. Likewise, to each lone pair we attribute a hydrogen-bonding acceptor strength determined by the topological context of the acceptor atom. Eventually, in force-field calculations, the product of the hydrogen-bonding strengths for two atoms forming a hydrogen bond will determine the energy stored in this interaction.

The parameters entering the hydrogen-bonding donor- and acceptor strengths of polar atoms are adjusted so that we can optimally reproduce the Gibbs free energy of hydration of a molecule by assuming that each polar atom contributes via simple functions of its hydrogen-bonding strengths.

Hydrogen-bonding donor strength

Hydrogen partial atomic charges q_H offer themselves as primary candidates for the donor strengths. Their values can be directly obtained from the charge distribution calculation of the previous sections. For the case of strictly united-atom calculations, in which also polar hydrogen atoms are absorbed in their respective heteroatoms (this is the standard case for MAB), it is straightforward to reconstruct the implicit hydrogen charges by accounting for the effect of the variables c_{HX} (charge shifts along H-X bonds) which have been eliminated from the full (all-atom) equations (Equation (1)).

In addition, we consider a modification to account, in a simple way, for the influence of charges from topological neighbors of the principal (hydrogen) atom. The effect of these charges is lumped together into a simple corrective charge of the form:

$$\delta q_i = T \sum_k^{nbr} q_k + T^2 \sum_k^{nnbr} q_k + T^3 \sum_k^{nnnbr} q_k. \qquad (9)$$

This expression accounts for a progressively reduced influence of the charges of increasingly distant neighboring atoms by a reduction factor which decreases exponentially with topological distance. The bond reduction factor T is treated as a free parameter which turned out to be optimally chosen as 0.274, indicating a rapid reduction of neighbor influences with (topological) distance. The total donor strength, s_d, is taken to be proportional to the neighbor-corrected hydrogen charge

$$s_d = D(q_H + \delta q_H) \qquad (10)$$

with the proportionality constant D.

Hydrogen-bonding acceptor strengths

H-bond acceptor atoms have a more complicated charge distribution than hydrogen atoms. Correspondingly, and in accordance with the inclusion of hybridization moments in evaluating dipole moments, we describe the acceptor strength of an atom i by three quantities, its corrected partial charge $q_i + \delta q_i$ (Equation (9)), its hybridization dipole $\mathbf{p}_{hi}$ (Equation (5)), and its quadrupole tensor $\mathbf{w}_i$. The atomic quadrupole moment $\mathbf{w}_i$ is built up as a sum of contributions of the occupied atomic valence orbitals. The bonding σ-orbitals yield

$$\mathbf{w}_i^\sigma = \sum_\beta^{\sigma-bonds} (1 - s_\beta^i)(1 - \Delta_\beta^i c_\beta)\mathbf{u}_\beta, \qquad (11)$$

where $\mathbf{u}_\beta$ is an axial unit tensor with its principal axis (of eigenvalue 1) along bond β and two equivalent perpendicular axes of eigenvalue –0.5.

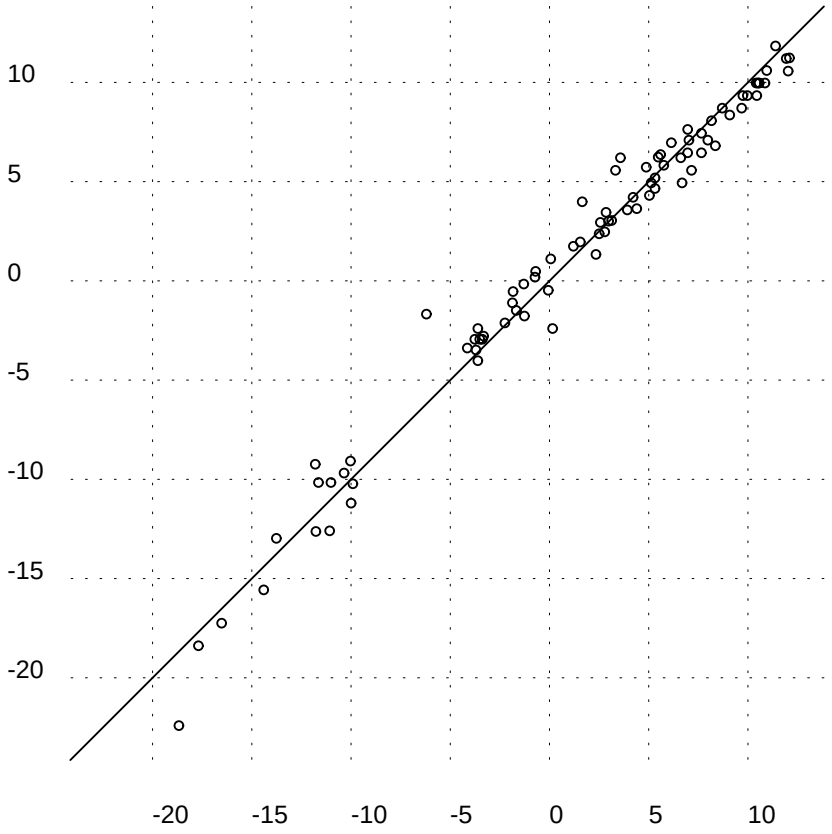

Figure 2. Calculated versus experimental free energies of hydration (in kJ/mol) for hydrocarbons. The model yields values with a confidence limit of 1.2 kJ/mol.

An analogous contribution $\mathbf{w}_\pi$ originates from the π-orbital(s) of the atom, if any, with the unit tensor $\mathbf{u}_\pi$ directed along the axis of the atomic π-orbital, with proper occupation numbers and, obviously, no reduction due to s-orbital content.

In addition there may be σ-lone pairs. Their contribution $\mathbf{w}_{LP}$, which is also of the form of Equation (11), depends on the content of atomic p-orbital of the lone-pair orbital, which also determines the direction of the corresponding unit tensors $\mathbf{u}_{LP}$.

For our purpose it is sufficient to determine the resulting total quadrupole moment only approximately by ignoring any possible asymmetry among the σ-bonds.

Collecting the contributions to the three acceptor terms (charge, dipole, and quadrupole), we consider the following (direction-dependent) acceptor variable

$$V_a(\mathbf{a}) = q_i + \delta q_i + A_p \mathbf{p}_{hi}\mathbf{a} + A_w \mathbf{w}_i \mathbf{a}\,\mathbf{a} \qquad (12)$$

in which $\mathbf{a}$ is the unit vector of the acceptor direction. Depending on the values of the parameters A_p and A_w the angular dependence shows distinct maxima. We take these maximum values, v_a, which, depending on the bonding geometry, may be assumed in one or two directions, to define a hydrogen-bond acceptor strength of the form

$$s_a = A v_a (A_0 + v_a). \qquad (13)$$

The functional form with the parameters A and $A_0 = 0.08$ ensures that s_a vanishes for $v_a = 0$, on the one hand, and allows for accelerated increase of s_a with increasing v_a, on the other hand. The number of lone pairs, n_{LPi}, is accordingly taken to be equal to the number of maxima, which conforms to the concept of lone pairs.

Polar part of the free energy of hydration

With the number of hydrogens n_H of a polar atom and the corresponding donor strength s_d, Equation (10), as

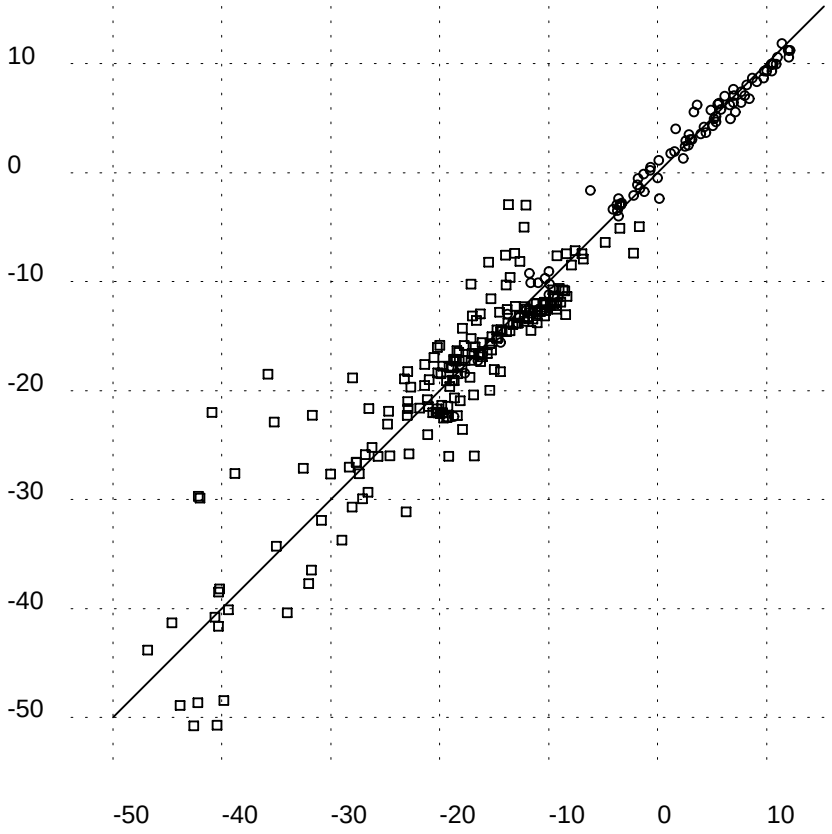

Figure 3. Calculated versus experimental free energies of hydration (in kJ/mol) for polar and non-polar compounds, including the ones of Figure 2. This more complete model yields values with a confidence limit of 3.5 kJ/mol.

well as the number of lone pairs n_{LP} and their acceptor strength s_a, Equation (13), we may proceed to formulate a polar contribution to the free energy of hydration of a molecule containing polar atoms.

$$\Delta G_h^p = g_d \sum_i^{\text{donors}} s_{di}(n_{Hi})^{0.68} + g_a \sum_i^{\text{acceptors}} s_{ai}(n_{LPi})^{0.51}, \quad (14)$$

where the exponents of the power laws were determined by fitting the experimental data. The power laws can be interpreted in terms of hydrogen-bonding strength attenuations by interaction in analogy to the terms introduced in the following paragraph. The quantities g_d and g_a are free parameters.

Interaction term

It has been found (see, e.g., [31]) that groups which contribute considerably to the Gibbs free energy of hydration influence each other when they are in close proximity, resulting in a reduction of the combined contribution [31]. We attempt to account for this effect by introducing the following simplistic correction term between topologically close atoms

$$\Delta G_h^i = g_i \left(\sum_k^{\text{bonds}} a_k^1 a_k^2 + \sum_k^{\text{nnbr}} a_k^1 a_k^2 + F \sum_k^{\text{nnnbr}} a_k^1 a_k^2 \right), \quad (15)$$

where a^i is given by

$$a^i = s_{ai}(n_{LPi})^{0.51} \quad (16)$$

i.e., the contribution of atom i entering the second sum of Equation (14). The index values $i = 1$ and 2 identify the two atoms in bonding-, next-nearest neighbor, and next-next-nearest neighbor contexts for the three sums over k, respectively.

The small value of F = 0.325, obtained from fitting to the experimental data, may be an indication that consideration of effects for larger distances is not sensible in this simplistic approximation. The justification of including this interaction term at all was to avoid the masking of the smaller contributions to Equation (14) by the most sizeable interaction contributions of Equation (15). Furthermore, as already mentioned, the nonlinear behaviour of donor and acceptor contributions which is expressed by the power-law behaviour in the multiplicities n_H or n_{LP} in Equation (14), may also be interpreted as a reduction by interaction, and thus, inclusion of ΔG_h^i may be considered a matter of consistency.

Comparison with experimental data

To describe the polar contributions to the Gibbs free energy of hydration we determined the parameters g_d, g_a, and g_i as well as the relative weights of monopolar, dipolar and quadrupolar acceptor contributions via the quantities A_p and A_w. Furthermore, values for the exponents in Equation (14) as well as for T (Equation (9)) and A_0 (Equation (13)) were optimized, by minimizing the root mean square deviations between experimental and calculated data. The parameters of Equation (7) were left unchanged and the corresponding descriptors were introduced for the polar atoms as well. The total set of 281 compounds considered is listed in the Table of Appendix 2. The coefficients g_d, g_a, and g_i as well as the constant g_0 (which was again left free) were the result of a linear regression analysis, while the remaining parameters, in particular the weights A_p and A_w, which enter non-linearly in Equation (14), were adjusted in a step by step process. The value of g_0 from the whole set of compounds remained at 5.16 ± 0.36 kJ/mol, in good agreement with the value determined from the hydrocarbons alone.

The parameters D (Equation (10)) and A (Equation (12)) are redundant for the least-square fitting since they can be absorbed in the values of g_d and g_a, Equation (14), respectively. They are set to one in the following. However, when using donor and acceptor strengths to model non-bonded interactions in our force field, they are useful to set the energy scale and the relative weight of donor and acceptor terms (see next section).

The most important parameters in the context of this work are the ones describing the hydrogen-bonding effects. The regression analysis yielded the values $g_d = -139 \pm 6$ kJ/mol, $g_a = -32.0 \pm 0.8$ kJ/mol, and $g_i = 37.2 \pm 2.0$ kJ/mol, when the mutually optimized quantities assumed the values $A_p = 0.56$ and $A_w = 0.64$. With these values the experimental data, which span a range of -13.0 ± 12.7 (rmsd) kJ/mol, could be reproduced with a root mean square deviation of 3.5 kJ/mol. This compares not unfavorably with other models (5.5 and 4.6 kJ/mol in [32] and [33] respectively on a less complete set of data). This is a rather satisfactory agreement. The very narrow uncertainty limits of the g-parameters may indicate that the concept of hydrogen-bonding donor and acceptor strengths of polar atoms is a valid model description for Gibbs free energies of hydration.

For only few compounds containing second-row elements data were available. For this reason we excluded these compounds from the fit and calculated their values with the parameters (A_p and A_w) from the first row compounds, with reasonable success, as shown in the table of Appendix 2.

Figure 2 displays the calculated values versus the experimental ones. While the overall agreement is rather satisfactory, there are a few significant outliers, most prominently, the N-alkyl-substituted amides. These compounds show, rather conspicuously, Gibbs free energies of hydration very similar to the non-substituted ones, despite the reduced number of hydrogens. However, we postpone to future work any fine tuning of the hydration model. Likewise, we have not included halogenated compounds for the reason that halogens are not considered hydrogen-bond acceptors in our force field MAB.

MAB force-field parameters for hydrogen bonding

We can now make use of these results to parametrize the non-bonded interactions for our force field MAB. The absolute energy of a hydrogen bond is given by a product of donor- and acceptor-specific hydrogen-bonding strengths, modulated by a geometrical expression given by distance and directional terms of donor and acceptor heavy atoms. In previous versions, the parametrization step assigned hydrogen-bonding donor or acceptor strengths purely on the basis of generic atom types for the heavy atoms, determined only by the position of the atom in the periodic table. Such a parametrization was unable to account for the considerable variation encountered for the same atom in various chemical contexts. The experimentally parametrized model of hydration presented here provides a basis for assigning topology dependent atomic hydrogen-bonding donor and acceptor strengths.

The quantities s_{di} (Equation (10)) and s_{ak} (Equation (13)) are used to parametrize the strength of a hydrogen bond between atom i as the donor and atom k as the acceptor. The parameters $D = 63.7$ and $A = 9.74$ (in units of $(kJ/mol)^{0.5}$) are chosen so as to yield an identical donor and acceptor strength of 4.77 $(kJ/mol)^{0.5}$ for the water molecule, as well as a water–water hydrogen-bond energy of 22.8 kJ/mol [34]. With this convention we also obtain normalized values for the constants g_d and g_a which we call $\gamma_d = g_d/D$ and $\gamma_a = g_a/A$. They have the values -2.18 and –3.29 $(kJ/mol)^{0.5}$ respectively.

The two numbers γ_d and γ_a indicate that the contribution of hydrogen bonding to the Gibbs free energy of solvation for a single-valued donor or acceptor is about one half or two thirds, respectively, of the energy of the corresponding isolated hydrogen bond to a single water molecule.

For ammonia we obtain the pair (2.20, 6.60) for donor and acceptor strength, while for hydrogen-fluoride the pair is (7.47, 1.67) (all numbers in $(kJ/mol)^{0.5}$). This illustrates the weak acceptor properties of halogens which led us to ignore them to start with. By multiplying appropriate donor and acceptor strengths one obtains directly MAB estimates for the binding energies of the linear-hydrogen-bond complexes of the corresponding first row hydrides. The resulting values of 12.5 and 14.5 kJ/mol for $(HF)_2$ and $(NH_3)_2$, respectively, agree reasonably well with the corresponding experimental values of 12.7 [35] and 11.7 [36].

In this context it is also of interest to see how large donor strength values are predicted for carbon atoms, even though they are neglected in present MAB calculations. We obtain values of 0.47, 1.09, 1.45, and 4.03 $(kJ/mol)^{0.5}$ for ethane, ethene, benzene, and ethyne respectively. Clearly, omitting ethyne donor properties can only be justified by the rare occurrence of this group, while sp_2-carbon values are at most of marginal importance.

Conclusions

A few comments may be in order here relating to the description of intermolecular interactions in terms of atom-centered partial charges interacting via the Coulomb law. Such a treatment is now standard in molecular mechanics calculations and considerable effort is spent on dealing with the associated long-range problems [37]. The quantities of primary interest in comparing our treatment with a point-charge description are the bond reduction parameter T, Equation (9), and the multipole weights A_p and A_w, Equation (12).

The surprisingly small value of T may be interpreted as an indication that short-range effects may have to supplement a description of hydrogen bonds in terms of interacting atom-centered charges. Theoretical investigations have uncovered short-range penetration contributions to intermolecular interaction [17] which appear to be of similar nature. This may also be in line with the marked directionality found in experimental analyses. Pronounced directionality is also an indication for the presence of short range forces.

Furthermore, one can also obtain estimates for A_p and A_w under the assumption of a pure electrostatic interaction of the corresponding charge multipoles. An estimate for A_p can be obtained by assuming a hydrogen-bond distance of 1.8 Å and a typical van der Waals radius for polar first row atoms of 1.7 Å. Thus, with the value $P_h = 0.275$ (see after Equation (5)) the dipolar contribution is expected to be smaller by a factor of 0.26 compared to the monopolar contribution. This seems somewhat low when compared to $A_p = 0.56$. For the quadrupolar interaction we have no experimental value for the quantity P_w which, in analogy to P_h, relates the quadrupole moment of a p-orbital to the square of the atomic van der Waals radius. From hydrogen-type wave functions we estimate a value of $P_w = 0.12$. This indicates that the interaction energy of a donor charge with the quadrupole moment of a p-orbital electron would be lower by roughly a factor 0.21 when compared to the interaction with a unit charge at the center of the acceptor atom. This is considerably lower than the value of $A_w = 0.64$. In essence, the influence of higher multipole moments on acceptor strengths increases as if the donor charge was positioned at only about 0.6 times its actual distance! Although this finding has to be put into perspective by the fact that the donor strengths include neighborhood charges (Equation (9)) which interact relatively more strongly with the lower moments than with the higher ones, the corresponding correction appears to be of moderate importance, owing to the small value of T in Equation (9). Thus again, the large values of A_p and A_w indicate that charge distributions on small intra-atomic scales appear to be of high importance for intermolecular interactions. This may again be rephrased to indicate the predominance of short-range interactions [17].

Hydrogen-bonding strengths of different experimental origin have been used to describe various

physicochemical and pharmacological properties of molecules [38,39]. It remains to be seen how useful the strengths presented here turn out to be in this respect.

In summary, we have presented a model for the free energy of hydration in terms of hydrogen-bond donor and acceptor properties of polar groups. The resulting donor and acceptor strength are used to parametrize our force field MAB, which employs explicit short-range directional hydrogen bonding terms in place of the conventional Coulomb-law interactions of atom-centered partial charges. The experimentally supported importance of high multipole moments of the atomic charge distribution in finding these strengths is a direct support of the concept of directionality dependence of hydrogen bonding.

Acknowledgements

This work has considerably profited from discussions with F. Winkler, M. Kansy, J. Boehm, and S. Fischer. Valuable comments on the manuscript by K. Muller are gratefully acknowledged.

References

1. Li, J.H. and Allinger, N.L., J. Comput. Chem., 12 (1991) 186.
2. Brooks, B.R., Bruccoleri, R.E., Olafson, B.D., States, D.J., Swaminathan, S. and Karplus, M., J. Comput. Chem., 4 (1983) 187.
3. Momany, F.A., McGuire, R.F., Burgess, A.W. and Scheraga, H.A., J. Phys. Chem., 79 (1975) 2361.
4. Weiner, S.J., Kollman, P.A., Case, D.A., Singh, U.C., Ghio, C., Alagona, G., Profeta Jr., S. and Weiner, P., J. Am. Chem. Soc., 106 (1984) 765.
5. van Gunsteren, W.F. and Berendsen, H.J.C., GROMOS Library Manual, Biomos (1987) Nijenborgh 16, 9747 AG Groningen, The Netherlands.
6. Maple, J.R., Dinur, U. and Hagler, A.T., Proc. Natl. Acad. Sci. USA, 85 (1988) 5350.
7. Clark, M., Cramer III, R.D. and van Opdenbosch, N., J. Comput. Chem., 10 (1989) 982.
8. Momany, F.A. and Rone, R., J. Comput. Chem., 13 (1992) 888.
9. Breneman, C.M. and Wiberg, K.B., J. Comput. Chem., 11 (1989) 361.
10. Gasteiger, J. and Marsili, M., Tetrahedron, 36 (1980) 3219.
11. Gasteiger, J. and Saller, H., Angew. Chem. Int. Ed. Engl., 24 (1985) 687.
12. Rappé, A.K. and Goddard III, A., J. Phys. Chem., 95 (1991) 3358.
13. Winkler, R. and Pantelides, S.T., J. Chem. Phys., 106 (1997) 7714.
14. Abraham, R.J. and Grant, G.H., J. Comput.-Aided Mol. Design, 6 (1992) 273, and references therein.
15. Abraham, R.J., Warne, M.A. and Griffiths, L., J. Chem. Soc. Perkin Trans. 2, (1997) 881.
16. Lommerse, J.P.M., Price, S.L. and Taylor, R., J. Comput. Chem., 18 (1997) 757.
17. Wheatley, R.J. and Michell, J.O.B., J. Comput. Chem., 15 (1994) 1187.
18. Kollmann, P.A., J. Am. Chem. Soc., 100 (1978) 2974.
19. Vedani, A. and Dunitz, J.D., J. Am. Chem. Soc., 107 (1985) 7653.
20. Vinter, J.G., J. Comput.-Aided Mol. Design, 8 (1994) 653.
21. Vinter, J.G., J. Comput.-Aided Mol. Design, 8 (1996) 417.
22. Gerber, P. and Muller, K., J. Comput.-Aided Mol. Design, 6 (1995) 251.
23. Heilbronner, E. and Bock, H., The HMO Model and its Application, John Wiley & Sons, London, 1976.
24. Hinze, J., Whitehead, M.A. and Jaffé, H.H., J. Am. Chem. Soc., 85 (1963) 148.
25. Hinze, J. and Jaffé, H.H., J. Am. Chem. Soc., 84 (1962) 540.
26. Streitwieser, A., Molecular Orbital Theory for Organic Chemists, John Wiley, New York, NY, 1961.
27. Dewar, M.J.S., The Molecular Orbital Theory of Organic Chemistry, McGraw-Hill, New York, NY, 1969.
28. Callomon, J.H., Hirota, E., Kuchitsu, K., Lafferty, W.J., Maki, A.G. and Pote, C.S., In Hellwege, K.H. (Ed.) 'Landold-Boernstein', Vol.7, 'Strukturdaten Freier Mehratomiger Molekeln', Springer, Berlin, 1976.
29. McClellan, W.H., Tables of Experimental Dipole Moments, Freeman, San Francisco, CA, 1963.
30. Marynick, D.S., J. Comput. Chem., 18 (1997) 955.
31. Cabani, S., Gianni, P., Mollica, V. and Lepori, L., J. Sol. Chem., 10 (1981) 563.
32. Ooi, T., Oobatake, M., Nemethy, G. and Scheraga, H.A., Proc. Natl. Acad. Sci. USA, 84 (1987) 3086.
33. Ulmschneider, M., Ph. D. Thesis (1993). Université de Haute-Alsace, Strasbourg, France.
34. Curtiss, L.A., Frurip, D.J. and Blander, M., J. Chem. Phys., 71 (1979) 2703.
35. Quack, M. and Suhm, M.A., Theor. Chim. Acta, 93 (1996) 61.
36. Nelson, D.D., Fraser, G.T. and Klemperer, W., J. Chem. Phys., 87 (1985) 6364.
37. Berne, B.J. and Straub, J.E., Curr. Opin. Struct. Biol., 7 (1997) 181.
38. Raevsky, O.A., Grigorev, V.Y., Kireev, D.B. and Zefirov, N.S., Quant. Struct.-Act. Relatsh., 11 (1992) 49.
39. Raevsky, O.A., In Van de Waterbeemd H., Testa, B. and Folkers, G. (Eds.) Computer-Assisted Lead Finding and Optimization, Helvetica Chimica Acta, Basel, 1997, p. 367..
40. Wolfenden, R., Andersson, L., Cullis, P.M. and Southgate, C.C.B., Biochemistry, 20 (1981) 849.
41. Cullis, P.M. and Wolfenden, R., Biochemistry, 20 (1981) 3024.
42. Wolfenden, R., Liang, Y., Matthews, M. and Williams, R., J. Am. Chem. Soc., 109 (1987) 463.
43. Wolfenden, R. and Liang, Y., J. Biol. Chem., 263 (1988) 8022.
44. Gibbs, P.R., Radzicka, A. and Wolfenden, R., J. Am. Chem. Soc., 113 (1991) 4714.

Appendix 1. Dipole moments

Experimental and calculated dipole moments for a set of molecules with well defined geometries. Geometries are taken from [28] except in a few unambiguous cases, where force field minima were considered sufficiently reliable. Dipole moments, in Debye units, were taken from [29].

Structure	Exp.	Calc.	Diff.
Butane	0.00	0.00	0.00
Ethane	0.00	0.00	0.00
Propane	0.00	0.04	0.04
Dimethyl-ether	1.25	1.71	0.46
Ethanol	1.70	1.58	–0.12
Methanol	1.65	1.66	0.01
Methylamine	1.29	1.20	–0.09
Methyl-mercaptan	1.26	1.59	0.33
Methyl-phosphine	1.10	1.34	0.24
Dimethyl-disulfide	1.97	2.17	0.20
Dimethyl-sulfide	1.50	1.86	0.36
Dimethyl-sulfone	4.47	5.47	1.00
Dimethyl-sulfoxide	3.90	4.12	0.22
Benzene	0.00	0.00	0.00
Butadiene	0.00	0.00	0.00
2-Butene	0.00	0.00	0.00
Ethene	0.00	0.00	0.00
Hexatriene	0.00	0.00	0.00
Isobutene	0.00	0.14	0.14
Propene	0.34	0.07	–0.27
Methyl-formate	1.77	1.63	–0.14
Acetaldehyde	2.68	2.62	–0.06
Acetamide	3.70	3.70	0.00
Acetone	2.70	2.77	0.07
Acrolein	2.90	3.04	0.14
Aniline	1.55	0.96	–0.59
Anisole	1.20	1.54	0.34
Azomethane	0.00	0.00	0.00
Benzoquinone	0.00	0.00	0.00
Nitroethene	3.44	4.07	0.63
Phenol	1.60	1.31	–0.29
Allene	0.00	0.00	0.00
Ethine	0.00	0.00	0.00
Propine	0.75	0.25	–0.50
Phenyl-isocyanide	3.56	3.22	–0.34
Acrylonitrile	3.50	3.31	–0.19
Benzonitrile	3.90	3.53	–0.37
trans-N-methyl-acetamide	4.30	3.68	–0.62
Methyl-isothiocyanate	3.59	2.73	–0.86
Cyclopentadiene	0.47	0.18	–0.29
Fluorene	0.50	0.16	–0.34
Fulvene	1.10	1.36	0.26
Ethylene-epoxide	1.90	1.95	0.05
Furan	0.65	0.31	–0.34
Imidazole	3.87	3.68	–0.19
Indole	2.10	1.74	–0.36
Pyrazole	1.60	2.23	0.63
Pyridine	2.30	2.11	–0.19
Pyrrole	1.80	1.76	–0.04
Thiazole	1.65	1.90	0.25
Thiophene	0.51	0.12	–0.39
Bicyclo[1.1.1]pentane	0.00	0.00	0.00
Cyclobutane	0.00	0.00	0.00
1,3-Cyclohexadiene	0.38	0.13	–0.25
Cyclohexene	0.61	0.00	–0.61
Cyclooctatetraene	0.00	0.01	0.01
Cyclopropane	0.00	0.00	0.00
Cyclopentene	0.95	0.25	–0.70
Spiropentane	0.00	0.00	0.00
Cyclopropylchloride	1.78	0.98	–0.80
Oxetane	1.93	1.92	–0.01
Thietane	1.78	2.01	0.23
Hydrocyanide	2.95	2.67	–0.28
Trimethyl-amine	0.86	1.18	0.32
Trimethyl-phosphine	1.19	1.98	0.79
Dimethyl-amine	1.00	1.21	0.21
Dimethyl-ketene	1.85	1.95	0.10
Dimethyl-nitramine	4.61	4.32	–0.29
Dimethyl-nitrosamine	4.01	3.40	–0.61
Methyl-cyanide	3.97	3.18	–0.79
Methyl-isocyanide	3.80	3.18	–0.62
Methyl-nitrate	3.10	3.74	0.64
Methoxy-ethyne	1.81	1.82	0.01
Methyl-thiocyanate	3.34	3.23	–0.11
Acetylchloride	2.71	3.03	0.32
Acetylcyanide	3.45	3.10	–0.35
Acetylfluoride	2.96	2.93	–0.03
Aziridine	1.89	1.29	–0.60
Cyclobutanone	2.61	3.15	0.54
Chloroacetylene	0.44	0.56	0.12

Structure	Exp.	Calc.	Diff.
Cyclopropene	0.45	0.26	–0.19
Cyanoacetylene	3.60	3.27	–0.33
Fluoroacetylene	0.75	1.34	0.59
Ketene	1.40	1.73	0.33
Maleic anhydride	3.94	3.97	0.03
Methacrylonitrile	3.69	3.29	–0.40
Nitromethane	3.46	3.94	0.48
Vinylchloride	1.44	0.94	–0.50
Vinylfluoride	1.43	1.46	0.03
Methyl-benzoate	1.85	1.93	0.08
N,*N*-dimethyl-acetamide	3.81	3.81	0.00
Acetic acid	1.30	1.89	0.59
Acetonitrile	3.50	3.18	–0.32
Acetophenone	2.90	3.06	0.16
Ammonia	1.47	1.30	–0.17
Benzamide	3.65	3.82	0.17
Benzophenone	2.97	3.24	0.27
Cyclohexanol	1.80	1.76	–0.04
Chlorobenzene	1.55	0.71	–0.84
Chloroethane	2.00	1.34	–0.66
Chloromethane	1.69	1.30	–0.39

Structure	Exp.	Calc.	Diff.
Ethylacetate	1.85	1.87	0.02
Ethylamine	1.30	1.20	–0.10
Ethyleneoxide	1.90	1.90	0.00
Fluorobenzene	1.50	1.49	–0.01
Fluoromethane	1.79	1.70	–0.09
Formamide	3.40	3.48	0.08
Water	1.85	1.54	–0.31
Hydrogen fluoride	1.74	1.21	–0.53
Nitrobenzene	4.00	4.52	0.52
Pyridazine	3.97	3.85	–0.12
Pyridine-*N*-oxide	4.24	4.71	0.47
Pyrimidine	2.00	2.17	0.17
Quinoline	2.10	2.11	0.01
s-Trioxane	2.20	3.10	0.90
Styrene	0.10	0.06	–0.04
Tetrahydrofuran	1.70	1.83	0.13
Thiourea	4.93	4.17	–0.76
Toluene	0.40	0.08	–0.32
Urea	4.56	4.28	–0.28
Sigma, avg. diff.	2.351	0.360	–0.047

Appendix 2. Free energy of hydration

Experimental free energies of hydration (in kJ/mol) for a list of compounds. Most values were taken from the standard compilation by Cabani et al. [31]. Later measurements are explicitly referenced. Also shown are calculated values and deviations. Some data were excluded from the fit due to possible occurrence of internal hydrogen bonds[a], second row elements[b] (see text), or just a suspicious value[c].

Structure	Exp.	Calc.	Diff.	Ref.
Methane	8.37	6.44	–1.92	
Ethane	7.66	7.08	–0.58	
Propane	8.18	7.71	–0.47	
Butane	8.70	8.34	–0.35	
2-Methyl-propane	9.70	8.34	–1.35	
Pentane	9.76	8.97	–0.78	
Methyl-butane	9.97	8.97	–0.99	
Dimethyl-propane	10.46	8.97	–1.48	
Hexane	10.40	9.61	–0.79	
2-Methyl-pentane	10.56	9.61	–0.95	
3-Methyl-pentane	10.50	9.61	–0.89	
2,2-Dimethyl-butane	10.85	9.61	–1.24	
Heptane	10.96	10.24	–0.72	
2,4-Dimethyl-pentane	12.04	10.23	–1.81	
Octane	12.10	10.87	–1.22	
2,2,4-Trimethyl-pentane	11.93	10.86	–1.06	
2,2,5-Trimethyl-hexane	11.39	11.50	0.10	
Cyclopropane	3.13	2.68	–0.44	
Cyclopentane	5.02	3.95	–1.07	
Cyclohexane	5.14	4.58	–0.55	
Methyl-cyclopentane	6.68	4.58	–2.09	
Cycloheptane	3.33	5.22	1.88	
Methyl-cyclohexane	7.14	5.22	–1.92	
Cyclooctane	3.58	5.85	2.27	
cis-1,2-Dimethyl-cyclohexane	6.62	5.85	–0.77	
Ethene	5.32	4.30	–1.02	
Propene	5.31	4.83	–0.48	
1-Butene	5.77	5.46	–0.30	
Methyl-propene	4.87	5.36	0.49	
1-Pentene	6.96	6.09	–0.86	
trans-2-Pentene	5.59	6.00	0.40	
2-Methyl-2-butene	5.48	5.89	0.41	
3-Methyl-1-butene	7.65	6.10	–1.55	
1-Hexene	7.02	6.73	–0.29	

Structure	Exp.	Calc.	Diff.	Ref.
2-Methyl-1-pentene	6.15	6.62	0.47	
4-Methyl-1-pentene	7.99	6.73	–1.26	
trans-2-Heptene	6.96	7.26	0.30	
1-Octene	9.08	7.99	–1.08	
Cyclopentene	2.34	0.97	–1.37	
Cyclohexene	1.54	1.60	0.06	
1-Methyl-cyclohexene	2.80	2.13	–0.66	
Butadiene	2.57	2.58	0.01	
1,4-Pentadiene	3.94	3.22	–0.72	
Cyclopentadiene	–6.20	–2.01	4.18	42
Methyl-butadiene	2.85	3.12	0.26	
1,5-Hexadiene	4.22	3.85	–0.37	
Dimethyl-butadiene	1.66	3.65	1.98	
Cycloheptatriene	–4.14	–3.73	0.41	
Ethine	–0.05	–0.83	–0.77	
Propine	–1.28	–0.51	0.76	
1-Butine	–0.68	0.12	0.80	
1-Pentine	0.06	0.75	0.69	
1-Hexine	1.20	1.39	0.18	
1-Heptine	2.51	2.02	–0.49	
1-Octine	2.97	2.65	–0.32	
1-Nonine	4.40	3.28	–1.11	
1-Buten-3-ine	0.17	–2.76	–2.92	
Benzene	–3.62	–4.36	–0.74	
Methyl-benzene	–3.71	–3.83	–0.11	
Ethyl-benzene	–3.33	–3.14	0.19	
1,2-Dimethyl-benzene	–3.77	–3.30	0.47	
1,3-Dimethyl-benzene	–3.50	–3.30	0.20	
1,4-Dimethyl-benzene	–3.37	–3.30	0.07	
Propyl-benzene	–2.23	–2.47	–0.24	
Isopropyl-benzene	–1.26	–2.12	–0.86	
1,2,4-Trimethyl-benzene	–3.60	–2.76	0.83	
Butyl-benzene	–1.66	–1.83	–0.17	
sec-Butyl-benzene	–1.88	–1.45	0.43	
t-Butyl-benzene	–1.83	–0.90	0.93	
t-Pentyl-benzene	–0.74	–0.14	0.59	
Biphenyl	–11.06	–12.95	–1.88	
Diphenyl-methane	–11.78	–12.96	–1.18	
Fluorene	–14.41	–15.92	–1.51	
Naphthalene	–10.01	–11.55	–1.54	
1-Methyl-naphthalene	–9.91	–10.57	–0.66	
1-Ethyl-naphthalene	–10.02	–9.44	0.57	
1,3-Dimethyl-naphthalene	–10.35	–10.04	0.30	
1,4-Dimethyl-naphthalene	–11.79	–9.59	2.20	

Structure	Exp.	Calc.	Diff.	Ref.
2,3-Dimethyl-naphthalene	–11.64	–10.49	1.14	
2,6-Dimethyl-naphthalene	–11.00	–10.49	0.50	
Acenaphthene	–13.77	–13.32	0.44	
Anthracene	–17.70	–18.75	–1.04	
Phenanthrene	–16.53	–17.60	–1.06	
Pyrene	–18.68	–22.77	–4.08	
Methanol	–21.40	–19.62	1.78	
Ethanol	–20.98	–19.10	1.88	
1-Propanol	–20.19	–18.48	1.70	
2-Propanol	–19.90	–18.58	1.31	
1-Butanol	–19.73	–17.87	1.86	
2-Methyl-1-propanol	–18.93	–17.87	1.05	
2-Butanol	–19.15	–17.97	1.17	
2-Methyl-2-propanol	–18.89	–18.07	0.81	
1-Pentanol	–18.72	–17.23	1.48	
3-Methyl-1-butanol	–18.50	–17.26	1.24	
2-Pentanol	–18.72	–17.35	1.36	
3-Pentanol	–18.22	–17.36	0.86	
2-Methyl-2-butanol	–18.54	–17.46	1.08	
1-Hexanol	–18.26	–16.60	1.65	
2,3-Dimethyl-2-butanol	–16.38	–16.85	–0.47	
3-Hexanol	–17.05	–16.74	0.30	
4-Methyl-2-pentanol	–15.64	–16.73	–1.09	
2-Methyl-3-pentanol	–16.26	–16.74	–0.48	
2-Methyl-2-pentanol	–16.44	–16.84	–0.39	
1-Heptanol	–17.76	–15.97	1.79	
4-Heptanol	–16.76	–16.12	0.63	
1-Octanol	–17.13	–15.33	1.79	
2-Propen-1-ol	–21.06	–21.57	–0.50	
Cyclopentanol	–22.99	–22.41	0.58	
Cyclohexanol	–22.91	–21.78	1.13	
Cycloheptanol	–22.95	–21.14	1.81	
Phenol	–27.68	–26.27	1.41	
2-Methyl-phenol	–24.58	–25.69	–1.11	
4-Methyl-phenol	–25.67	–25.74	–0.06	
4-*t*-Butyl-phenol	–24.79	–22.77	2.02	
Dimethyl-ether	–7.93	–8.36	–0.42	
Diethyl-ether	–6.84	–7.85	–1.00	
Methyl-propyl-ether	–6.96	–7.34	–0.37	
Methyl-2-propyl-ether	–8.39	–7.34	1.04	
Ethyl-propyl-ether	–7.59	–7.08	0.50	
Methyl-*t*-butyl-ether	–9.25	–7.56	1.68	
Dipropyl-ether	–4.83	–6.32	–1.48	
Di(2-propyl)-ether	–2.23	–7.34	–5.11	

Structure	Exp.	Calc.	Diff.	Ref.
Dibutyl-ether	–3.48	–5.03	–1.54	
Tetrahydrofuran	–14.52	–12.73	1.79	
2,3-Dihydropyran	–9.02	–7.51	1.50	43
Tetrahydropyran	–13.07	–12.19	0.88	43
2-Methyl-tetrahydrofuran	–13.82	–12.48	1.33	
2,5-Dimethyl-tetrahydrofuran	–12.22	–12.24	–0.02	
Methoxy-benzene	–4.34	–11.55	–7.20	
Dimethyl-ketone	–16.12	–15.49	0.63	
Methyl-ethyl-ketone	–15.22	–14.95	0.27	
Methyl-1-propyl-ketone	–14.76	–14.33	0.43	
Diethyl-ketone	–14.28	–14.42	–0.13	
Methyl-2-propyl-ketone	–13.56	–14.42	–0.85	
Methyl-1-butyl-ketone	–13.76	–13.69	0.07	
Methyl-*i*-butyl-ketone	–12.81	–13.70	–0.89	
2-Heptanone	–12.72	–13.05	–0.33	
4-Heptanone	–12.24	–13.17	–0.93	
Di(2-propyl)-ketone	–11.46	–13.35	–1.88	
2-Octanone	–12.06	–12.42	–0.36	
2-Nonanone	–10.41	–11.79	–1.37	
5-Nonanone	–11.18	–11.89	–0.71	
2-Undecanone	–9.05	–10.52	–1.47	
Adamantanone	–18.66	–20.57	–1.91	
Acetophenone	–19.18	–25.94	–6.76	
Ethanal	–14.66	–14.94	–0.28	
Propanal	–14.40	–14.41	–0.01	
Butanal	–13.29	–13.78	–0.49	
Pentanal	–12.68	–13.14	–0.46	
Hexanal	–11.76	–12.51	–0.74	
Heptanal	–11.18	–11.88	–0.69	
Octanal	–9.58	–11.24	–1.66	
Nonanal	–8.69	–10.61	–1.91	
trans-2-Butenal	–17.68	–17.09	0.59	
trans-2-Hexenal	–15.40	–15.53	–0.13	
trans-2-Octenal	–14.40	–14.27	0.13	
trans,trans-2,4-Hexadienal	–19.39	–18.97	0.41	
Benzaldehyde	–16.84	–25.85	–9.00	
Ethanoic acid	–28.05	–30.92	–2.87	
Propanoic acid	–27.09	–30.18	–3.08	
Butanoic acid	–26.59	–29.56	–2.97	
Methyl-methoate	–11.64	–14.60	–2.95	
Ethyl-methoate	–11.07	–13.91	–2.83	
Methyl-ethanoate	–13.87	–14.81	–0.94	
Propyl-methoate	–10.39	–13.27	–2.87	

Structure	Exp.	Calc.	Diff.	Ref.
2-Propyl-methoate	–8.45	–13.16	–4.70	
Ethyl-ethanoate	–12.95	–14.05	–1.10	
Methyl-propanoate	–12.27	–13.89	–1.62	
i-Butyl-methoate	–9.30	–12.34	–3.03	
Propyl-ethanoate	–11.95	–13.43	–1.48	
2-Propyl-ethanoate	–11.07	–13.35	–2.27	
Ethyl-propanoate	–11.70	–13.13	–1.43	
Methyl-butanoate	–11.85	–13.62	–1.77	
(3′-Methyl-butyl)-methoate	–8.90	–11.99	–3.09	
Butyl-ethanoate	–10.67	–12.80	–2.12	
i-Butyl-ethanoate	–9.87	–12.40	–2.52	
Propyl-propanoate	–10.27	–12.86	–2.59	
2-Propyl-propanoate	–9.30	–12.76	–3.46	
Ethyl-butanoate	–10.44	–12.89	–2.44	
Methyl-pentanoate	–10.77	–12.98	–2.21	
Pentyl-ethanoate	–10.27	–12.17	–1.90	
(3′-Methyl-butyl)-ethanoate	–9.25	–12.17	–2.92	
Propyl-butanoate	–9.53	–12.24	–2.70	
Ethyl-pentanoate	–10.56	–12.25	–1.69	
Methyl-hexanoate	–10.41	–12.35	–1.93	
Hexyl-ethanoate	–9.47	–11.54	–2.06	
Pentyl-propanoate	–8.33	–11.60	–3.27	
Ethyl-heptanoate	–9.64	–10.99	–1.34	
Methyl-octanoate	–8.53	–11.08	–2.55	
Methyl-benzoate	–17.92	–23.84	–5.92	
Methyl-amine	–19.09	–19.76	–0.67	
Ethyl-amine	–18.84	–19.20	–0.36	
Propyl-amine	–18.37	–18.61	–0.24	
1-Butyl-amine	–17.97	–18.01	–0.03	
1-Pentyl-amine	–17.14	–17.38	–0.24	
1-Hexyl-amine	–16.87	–16.75	0.12	
Dimethyl-amine	–17.93	–14.34	3.58	
Diethyl-amine	–17.02	–13.23	3.79	
Dipropyl-amine	–15.31	–11.64	3.66	
Dibutyl-amine	–13.92	–10.39	3.53	
Aziridine	–22.66	–19.72	2.93	
Azetidine	–23.25	–18.99	4.26	
Hexahydro-2H-azepine	–20.54	–17.04	3.49	
Octahydro-azocine	–18.43	–16.40	2.02	
Pyrrolidine	–22.94	–18.32	4.61	
Piperidine	–21.38	–17.67	3.70	
Trimethyl-amine	–13.55	–9.58	3.96	

Structure	Exp.	Calc.	Diff.	Ref.
Triethyl-amine	–12.65	–8.14	4.50	
1-Methyl-pyrrolidine	–16.65	–13.54	3.11	
1-Methyl-piperidine	–16.29	–12.94	3.34	
Aniline	–28.00	–18.89	9.11	
Pyrrole	–20.00	–15.89	4.10	42
1-Methyl-pyrrole	–12.10	–2.97	9.12	42
Pyridine	–19.66	–22.48	–2.82	41
2-Methyl-pyridine	–19.38	–22.45	–3.07	
3-Methyl-pyridine	–19.97	–22.06	–2.09	
4-Methyl-pyridine	–20.65	–22.00	–1.34	
2-Ethyl-pyridine	–18.13	–20.92	–2.79	
3-Ethyl-pyridine	–19.26	–21.40	–2.13	
4-Ethyl-pyridine	–19.82	–21.31	–1.48	
2,3-Dimethyl-pyridine	–20.19	–22.04	–1.84	
2,4-Dimethyl-pyridine	–20.35	–21.97	–1.61	
2,5-Dimethyl-pyridine	–19.74	–22.04	–2.29	
2,6-Dimethyl-pyridine	–19.25	–22.43	–3.17	
3,4-Dimethyl-pyridine	–21.84	–21.58	0.26	
3,5-Dimethyl-pyridine	–20.26	–21.65	–1.38	
4-*t*-Butyl-pyridine	–18.68	–19.05	–0.37	
2,6-di-*t*-Butyl-pyridine	–1.70	–4.97	–3.26	
3-Methyl-indole	–24.70	–21.95	2.75	
Ethyl-nitrile	–16.26	–17.23	–0.96	
Propyl-nitrile	–16.09	–16.79	–0.69	
Butyl-nitrile	–15.25	–16.17	–0.92	
Acetamide	–40.63	–40.90	–0.26	
Propyl-amide	–39.40	–40.22	–0.82	
N-Methyl-acetamide	–42.16	–29.78	12.38	
N,*N*-Dimethyl-acetamide	–35.77	–18.54	17.23	
N-Butyl-acetamide	–38.80	–27.68	11.12	
N-Acetyl-pyrrolidine	–40.90	–22.05	18.85	44
1-Methyl-guanidine	–46.80	–44.12	2.68	40
Imidazole	–40.30	–38.60	1.70	42
1-Methyl-imidazole	–35.20	–22.95	12.25	42
4-Methyl-imidazole	–40.20	–38.34	1.86	42
Nitroethane	–15.52	–8.30	7.22	
1-Nitropropane	–13.98	–7.64	6.33	
2-Nitropropane	–13.13	–7.47	5.65	
Nitrobenzene	–17.23	–18.86	–1.63	
2-Nitrotoluene	–15.01	–18.13	–3.12	
3-Nitrotoluene	–14.44	–18.32	–3.87	
1,2-Ethanediol	–32.03	–37.79	–5.76	
1,2,3-Propanetriol [a]	–38.56	–56.21	–17.64	
Dimethoxy-methane	–12.27	–4.97	7.29	

Structure	Exp.	Calc.	Diff.	Ref.
1,2-Dimethoxy-ethane	–20.23	–15.84	4.39	
1,1-Diethoxy-ethane	–13.70	–2.91	10.78	
1,2-Diethoxy-ethane	–14.78	–15.05	–0.27	
1,3-Dioxolane	–17.14	–10.18	6.95	
1,4-Dioxane	–21.15	–20.58	0.57	
1,2-Ethane-diamine	–31.78	–36.60	–4.81	
Piperazine	–30.86	–31.94	–1.08	
1-Methyl-piperazine	–32.53	–27.10	5.42	
1,4-Dimethyl-piperazine	–31.70	–22.17	9.53	
2-Methyl-pyrazine	–23.09	–30.99	–7.89	
2-Ethyl-pyrazine	–22.83	–25.67	–2.83	
2-*i*-Butyl-pyrazine	–21.11	–23.92	–2.80	
2-Ethyl-3-methoxy-pyrazine	–18.39	–22.44	–4.04	
2-*i*-Butyl-3-methoxy-pyrazine	–15.41	–20.15	–4.73	
2-Methoxy-ethanol	–28.31	–26.99	1.32	
2-Ethoxy-ethanol	–27.64	–26.57	1.07	
2-Propoxy-ethanol	–26.84	–25.84	0.99	
2-Butoxy-ethanol	–26.22	–25.20	1.02	
2-Methoxy-ethyl-amine	–27.39	–27.63	–0.24	
3-Methoxy-propyl-amine	–28.98	–33.74	–4.76	
2-Methoxy-pyridine	–16.90	–20.48	–3.58	41
2-Amino-pyridine	–34.00	–40.46	–6.46	41
1-Methyl-2-pyridone	–42.00	–30.01	11.99	41
Morpholine	–30.02	–27.57	2.44	
4-Methyl-morpholine	–26.51	–21.50	5.00	
Quinone [c]	–24.20	–46.34	–22.14	42
Hydroquinone	–42.20	–48.06	–5.85	42
4-Methoxy-phenol	–35.00	–33.57	1.43	
2-Nitro-phenol [a]	–20.80	–40.54	–19.73	42
3-Nitro-phenol	–40.31	–41.37	–1.05	42
4-Nitro-phenol	–44.58	–41.05	3.53	42
3-Hydroxy-benzaldehyde	–39.81	–47.98	–8.16	
4-Hydroxy-benzaldehyde	–43.83	–48.45	–4.61	
3-Cyano-phenol	–40.44	–50.27	–9.82	
4-Cyano-phenol	–42.57	–50.33	–7.76	
Methyl-thiol [b]	–5.19	–12.62	–7.42	
Ethyl-thiol [b]	–5.42	–12.11	–6.69	
Benzene-thiol [b]	–10.67	–19.73	–9.06	
Dimethyl-sulfide [b]	–6.45	–9.03	–2.58	
Diethyl-sulfide [b]	–5.99	–7.94	–1.94	
Methyl-thiobenzene [b]	–11.42	–11.07	0.34	